ELSEVIER

Surface Science 415 (1998) 251–263

surface science

A near-edge X-ray absorption fine structure study of atomic layer epitaxy: the chemistry of the growth of CdS layers on ZnSe(100)

M. Han [a], Y. Luo [a], J.E. Moryl [a], R.M. Osgood, Jr.[a,*], J.G. Chen [b]

[a] *Columbia Radiation Laboratory, Columbia University, New York, NY 10027, USA*
[b] *Exxon Research and Engineering Company, Annandale, NJ 08801, USA*

Received 15 January 1998; accepted for publication 22 May 1998

Abstract

Atomic layer epitaxy (ALE) using a binary reaction sequence of the precursors dimethylcadmium (DMCd) and hydrogen sulfide (H_2S) is shown to produce epitaxial layers of CdS on a ZnSe(100) substrate. Near-edge X-ray adsorption fine structure (NEXAFS) spectra taken at the carbon K-edge and sulfur L-edge are consistent with a growth model based on self-limiting surface reactions and support a mechanism based on sequential surface ligand displacement. This evidence, combined with a TPD study, shows the presence of alternating methyl- and hydride-terminated surfaces, which are passivated to further uptake of Cd or S, respectively. Layer-by-layer growth of good quality CdS was confirmed by comparison of NEXAFS spectra of bulk CdS with our grown films.

Keywords: Atomic layer epitaxy (ALE); CdS; $(CH_3)_2Cd$; Heteroepitaxy; H_2S; Near-edge X-ray absorption fine structure (NEXAFS); Surface chemistry; Synchrotron radiation; Temperature programmed desorption (TPD); Thin film deposition; II–IV semiconductors surface chemistry; ZnSe(100)

1. Introduction

Atomic layer epitaxy (ALE) is an important technique for growing thin films of compound semiconductor materials with atomically defined thickness and uniformity [1]. One approach to the ALE process is to utilize molecular precursors to transport the elements to the substrate and provide atomic layer control of deposition. This control will be facilitated if self-limiting surface chemistry occurs during the deposition process. In general, the molecular precursor approach is most appropriate for binary compounds because a binary chemical vapor deposition reaction can easily be separated into two half-reactions [2,3]. Although the ALE growth of a variety of semiconductor materials has been demonstrated, it has not generally been viewed as an opportunity for surface chemical investigations. However, in a series of recent papers, George and collaborators [4,5] have used such a surface chemical approach to achieve atomic layer deposition of amorphous insulators by a sequence of self-terminating reactions. Their results show that the surface chemistry underlying the ALE process determines the characteristics and quality of the film, and provide insight into how the growth process might be optimized.

Recently our group has studied a model system for II–VI heteroepitaxy, e.g. CdS/ZnSe, in which

* Corresponding author. Fax: +1 212 8541909; e-mail: osgood@columbia.edu

0039-6028/98/$ – see front matter
PII: S0039-6028(98)00453-1

ALE conditions are achieved through the use of a binary reaction sequence comprised of the sequential room-temperature dosing of the gas-phase precursor molecules dimethylcadmium (DMCd) and hydrogen sulfide onto a ZnSe(100) substrate. In previous studies in our laboratory [6,7], AES, XPS and LEIS have been used to characterize the chemical composition of the grown layer at each stage of the growth process. The results showed this binary reaction sequence can result in self-limiting growth at each half step of the reaction sequence, in turn, leading to the growth of a single bilayer of CdS during each full reaction cycle. In addition, LEED was employed to study the resulting surface order, showing that a good quality CdS film was obtained [6]. Despite this initial work, little was learned about the identity of surface reaction species and their geometry after each half-reaction. A proposed mechanism for the binary reaction sequence, which is consistent with our previous work, is shown in Fig. 1.

This paper describes the use of near-edge X-ray absorption fine structure (NEXAFS) experiments in conjunction with temperature programmed reaction studies to determine the surface species and to understand their adsorption geometry at each stage of the growth process. NEXAFS is a particularly good probe for elucidating properties of surface species, yielding information on the surface composition, binding sites and adsorbate orientation [8,9]. For example, carbon K-edge spectra, taken following the first half-reaction of DMCd with a clean ZnSe substrate (see Fig. 1), should reveal the presence of surface carbon and C–H bonds. Similarly, sulfur L-edge features can probe H–S and metal–sulfide bonds following the second half-reaction and subsequent annealing cycles. Sulfur L-edge spectra also offer a considerable increase in resolution over K-edge measurement [9,10]. As a result, the presence and binding site of sulfur can be readily characterized via comparison of sulfur L-edge features. For example, we show below that the spectrum for a thick annealed epitaxial layer, i.e. after 10 binary deposition cycles, is identical to the published spectrum for a CdS crystal [11,12].

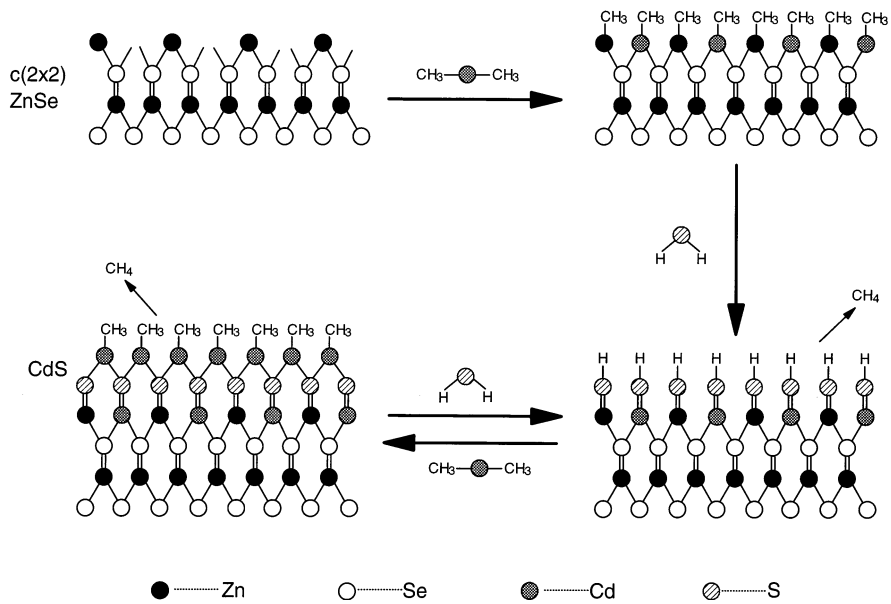

Fig. 1. Proposed mechanism for the ALE growth of CdS on a ZnSe(100)-c(2 × 2) surface. When DMCd is first supplied to the freshly prepared surface, Cd uptake occurs until a full monolayer of methyl groups cap the surface. Next, H_2S is supplied and methane is displaced and the sulfur uptake occurs until a complete hydrogen-terminated layer is obtained. Layer-by-layer growth is attained by continuing this dosing sequence.

2. Experimental

The experiments were conducted on the U1A Beamline of the National Synchrotron Light Source (NSLS) at the Brookhaven National Laboratory. Details of the experimental end station apparatus can be found in Ref. [13]. Experiments were performed in a two-level UHV chamber with a nominal base pressure of 5×10^{-10} Torr, equipped with an ion sputtering gun, an Auger electron spectrometer and a quadrupole mass spectrometer. The $5\,\text{mm}\times5\,\text{mm}$ ZnSe(100) sample was mounted on a molybdenum foil which was heated resistively and was capable of being cooled with liquid nitrogen. The sample temperature was measured with a chromel–alumel thermocouple welded onto the Mo foil. The precursors, i.e. DMCd (Strem Chemical, 99.999%) and H_2S (Matheson, 99.5%) were introduced to the growth surface via two separate dosing tubes located close to the surface; the flux of the precursor at the surface was controlled by separate leak valves and was monitored by measuring the pressure rise in the dosing chamber. Purity of the precursors was ensured by the use of freeze–pump–thaw cycles prior to each run.

The ZnSe(100) single-crystal substrate was prepared by sputtering at room temperature with 1000 eV Ar^+ ions followed by annealing at 415°C for 15 min and at 425°C for 3 min. This cleaning procedure produces a well ordered c(2×2) reconstruction which is a stable surface structure for II–VI materials terminated by a half monolayer of group II elements [14,15].

NEXAFS spectra were collected by measuring the partial electron yield using a channeltron electron multiplier. The incident X-ray energy was scanned from 275 to 325 eV for the carbon K-edge and from 150 to 200 eV for the sulfur L-edge, and the beam had a cross-section of $\sim4\,\text{mm}^2$. A bias voltage of -150 V for the carbon K-edge and -100 V for the sulfur $L_{II,III}$-edge were applied to a grid in front of the electron multiplier to provide a cutoff for low energy electrons. The resolution of the synchrotron monochromator was set at 0.25 and 0.20 eV for the carbon K-edge and the sulfur L-edge respectively. Spectra were taken at both glancing ($\theta=30°$, where θ is the angle between the direction of propagation of synchrotron light and the surface plane) and normal incidence ($\theta=90°$) for each growth stage. All spectra were first normalized by the incident light flux as monitored by an Au reference grid. Each of the NEXAFS spectra displayed below is taken at a particular stage of the growth process and then divided by a clean-surface spectrum taken at the same incident angle. Heights of the adsorption step edges, which are proportional to the amount of a given element on the surface, were compared for the same surface measured at different incidence angles and a normalization factor was obtained. The validity of such a treatment has been discussed previously [16].

3. Results and discussion

3.1. Carbon K-edge spectra of the adsorbed or grown surface layers

NEXAFS data at the carbon K-edge provide important information on the presence of carbon-containing species on the surface after each of the dosing steps and following surface annealing. Fig. 2 shows the carbon K-edge spectra taken at normal incidence for each of the first three steps of the growth sequence shown in Fig. 1, as well as a spectrum of physisorbed DMCd.

Fig. 2a is the spectrum for a multilayer of DMCd measured at liquid nitrogen temperature. Separate TPD measurements, discussed below, showed that low temperature dosing produces primarily unreacted physisorbed multilayers of DMCd, with some reaction apparently occurring in the molecules at the interface. Fig. 2a thus provides a calibration spectrum of the unreacted parent molecules, displaying a prominent near-edge structure peaked at 287.8 eV and a weaker shoulder at 285.5 eV. The origin of this latter feature is discussed below. A literature value for the carbon 1s ionization potential (IP) in DMCd was not found, but the carbon 1s IP values for gas-phase DMZn and DMHg are 289.3 and 289.7 eV, respectively [17]. Since the carbon 1s IP for DMCd should be similar, the peaks in our spectra then lie below the 1s IP, consistent with

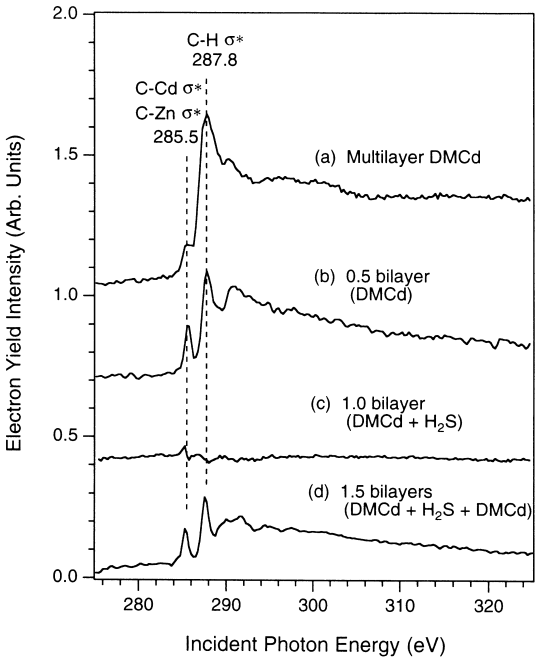

Fig. 2. Carbon K-edge NEXAFS spectra taken at various stages of the ALE growth of CdS on a ZnSe(100) substrate: (a) multilayer DMCd (precursor) spectrum, (b) spectrum taken after a clean substrate is exposed to a limiting dosage of DMCd, (c) clean substrate exposed to limiting dosages of DMCd and then H_2S, (d) clean substrate exposed to limiting dosages of DMCd, then H_2S and DMCd again. In the idealized reaction scheme, (b), (c) and (d) correspond to the last three stages of Fig. 1.

the sharpness of the NEXAFS features that are typically observed for transitions to bound states.

Fig. 2b displays a spectrum obtained after room-temperature dosing of DMCd onto the clean ZnSe substrate; a new feature is clearly evident when compared with the spectra of the physisorbed molecules. While there is a feature peaking at 287.8 eV, i.e. at the same energy as the major feature in the multilayer DMCd film, there is also a sharp new peak at 285.5 eV. As we will discuss below, this feature is most likely due to a transition to a molecular orbital associated with the metal–carbon bond in a monomethyl–metal surface moiety. Finally, in addition to the sharp features, the continuum level at the right edge of Fig. 2b is well above the baseline. The edge height provides a measure of the total amount of carbon in the near-surface region.

The third curve, Fig. 2c, shows the carbon K-edge spectrum after exposing the first monolayer metal–methyl terminated surface to H_2S at room temperature. In this case no detectable carbon K-edge features are observed; in addition the continuum level has "dropped back" to the baseline. These results clearly indicate that any carbon-containing groups are fully desorbed, most probably in the form of CH_4, after reaction with H_2S at room temperature.

Finally, the spectrum in Fig. 2d shows a spectrum from a saturated dosing of a one-bilayer "as-grown" surface with DMCd at room temperature. In our idealized model, the dosed surface should again be terminated with a full monolayer of methyl groups, each bonded to a substrate cadmium atom (third reaction step, Fig. 1). The spectrum shows the same two features, i.e. 285.5 and 287.8 eV, as observed after dosing a clean $c(2\times2)$ ZnSe(100) substrate with DMCd (Fig. 2b). This result indicates that DMCd reacts with the H_2S-dosed surface and that a monolayer of Cd is again deposited.

The same general trend is seen when reactive dosing is performed on a surface containing a large number of deposited bilayers. Specifically, the lower spectrum in Fig. 3 shows the NEXAFS

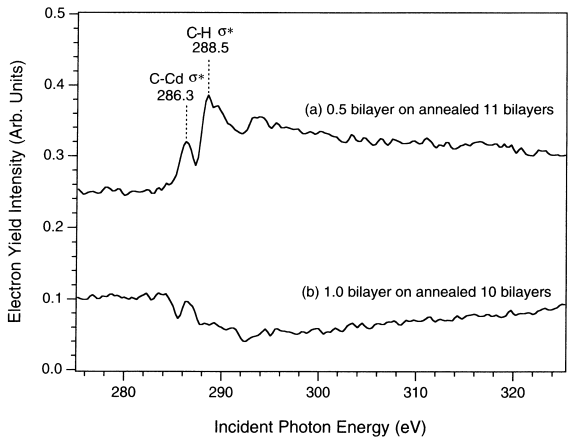

Fig. 3. Carbon K-edge NEXAFS spectra for precursors reacting with a thick epitaxial CdS layer. In (a) the spectrum is taken following exposure of the epilayer to DMCd and shows similar features to those in Fig. 2b and 2d. Spectrum (b) is surface prepared as in (a) but subsequently dosed with H_2S. The carbon K-edge features vanish, as in Fig. 2c.

carbon K-edge features following the growth of 10 full bilayers of CdS, annealing, and the further growth of another bilayer. Again no detectable carbon is seen, a result that is consistent with our Auger measurements, which also show no detectable carbon at this stage of the growth process. The surface was then annealed to 275°C and dosed with DMCd (top spectrum, Fig. 3); the carbon K-edge shows identical features to the spectrum in Fig. 2b and 2d, indicating that the grown CdS surface exhibits similar reactivity to that of a bare substrate. Note, however, the peaks are somewhat broader and with a higher noise level than those observed in the early stages of the growth process, suggesting that the surface order is less than that of a freshly prepared substrate.

Note that in Fig. 2d the height of the step edge following the third reaction step decreases slightly when compared with the apparently methyl-covered surface in Fig. 2b. While the present experiment does not allow us to rule out an explanation based on a reduced methyl concentration on the 1.5 bilayer surface compared to that on the 0.5 bilayer surface, recent TPD measurements in our laboratory do not support this explanation as no decrease of methyl concentration is observed as the growth proceeds to thicker layers [18]. However, a possible explanation is suggested by earlier LEED data which showed that surface roughness of the as-grown (not annealed) layers increases somewhat before the surface order recovers at the $\sim$10–15 bilayer level [19]. It is possible that increasing roughness can significantly influence the Auger electron emission by varying the cross-section of core–hole generation and the diffraction of the emitting electrons [20,21]. Since in this study the carbon K-edge X-ray absorption is indirectly measured by the emitted flux of carbon Auger electrons, it would be reasonable to attribute the decrease of carbon K-edge step height to an increase in the surface roughness.

In the absence of a series of experiments on well-known isolated or adsorbed molecular species, the unambiguous identification of NEXAFS features is difficult. However, careful cross-checking of experiments reported here as well as separate thermal desorption data allow us to narrow the possible origins of these features. Specifically, TPD measurements make it clear that room-temperature dosing does not result in *physisorbed* DMCd, and thus the two features, shown in Fig. 2b and 2d, originate from reacted chemisorbed precursors. Species formed could include CH_3 chemically bound to atoms incorporated into the surface, e.g. Cd–CH_3, Zn–CH_3 and possibly even Se–CH_3 or S–CH_3. In the case of the data taken on the thicker physisorbed layer, Fig. 2a, the spectral features would be expected to originate from transitions to C–H and Cd–C unoccupied σ^* orbitals in DMCd, with the latter perhaps possessing significant differences in molecular orbital energies and symmetry than the Cd–C σ^* resonance of monomethyl–metal species. It is not expected that any of the observed spectral features correspond to Rydberg states, which generally have insignificant intensity in condensed phase NEXAFS [8]. For the physisorbed spectra, any features originating from reactions at the interface (see below) should be greatly attenuated due to the limited escape depth for electrons moving through a physisorbed overlayer. The 287.8 eV features, observed in both physisorbed and reacted spectra, are in the region where transitions to the unoccupied orbitals associated with C–H bonds are commonly observed [8]. Assuming the validity of the building block picture for NEXAFS transitions, we assign these peaks to transitions arising from the presence of CH_3 groups, and note that this assignment is consistent with our TPD experiments where CH_3-containing species are observed to desorb from both physisorbed and reacted surfaces.

TPD spectra for DMCd adsorbed on the clean substrate at low temperature are shown in Fig. 4. The features near 160 K are due to the physisorbed overlayers, while those near 370 K we attribute to products originating from DMCd molecules in the near-surface layer that have reacted with the surface. Note that methyl groups appear to come from the surface mainly as fragments associated with zinc rather than cadmium.

The observation of the 285.5 eV peak following DMCd chemisorption is most readily interpreted as arising from a transition to a carbon–metal σ^* orbital associated with the methyl groups that are presumed to be capping a full metal monolayer. Other TPD studies have proposed the existence of

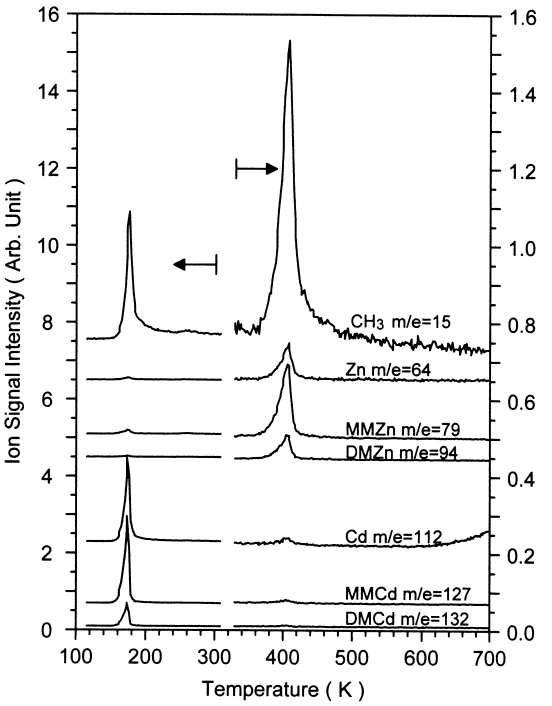

Fig. 4. TPD spectra following dosing of DMCd on a ZnSe c(2×2) surface at 100 K. Desorption of physisorbed DMCd occurs near 160 K and desorption of more strongly-bound species occur near 370 K.

surface monomethyl species following reactive dosing on both III–V and II–VI semiconductor surfaces [6,22]. Our proposed growth model begins with a half monolayer of methyl bound to Zn and another half monolayer bound to Cd; at the third growth step the entire monolayer should be bound to Cd. However, identical spectra are observed for DMCd reaction with either a bare or an "as-grown" surface, indicating that there is no chemical shift between C–Cd σ* and C–Zn σ*. This result is not unreasonable since Zn and Cd are in the same column of the periodic table, with similar values of electronegativity.

If a particular unoccupied σ* orbital can be primarily associated with a given X–C bond (where X is an element with a valence configuration of $2s^2 2p^n$, $n=2$–5), the position of the NEXAFS carbon K-edge transitions to this level can be correlated with the X–C bond length [8,23,24]. The usefulness of this correlation has been widely discussed in the literature [25], but in general the trend is well supported. For example, in CO the carbon 1s→σ* transition is a broad peak well above the IP; the equivalent transition for the longer C–F bond in CH_3F is much narrower and has moved to an energy below both the IP and C–H transitions [8]. The narrowness of the 285.5 eV peak and its position relative to the 287.8 eV feature we observe for the DMCd reacted on the surface (e.g. Fig. 2b) is qualitatively similar to the carbon K-edge spectra observed in methyl halides [26]. While the correlation between bond length and σ* resonance position is very strong for low Z atoms, the correlation, while still present, is not as well established when high Z atoms are involved [27]. It is not unreasonable to expect the nature of the C–Cd bond in DMCd to be quite different from the C–Cd bond in the surface species, which in our model has the surface Cd–CH_3 fragment bound to electronegative S or Se. If the bonding of the –Cd–CH_3 moiety with the surface results in a lengthening of the Cd–C bond, one would expect a shift in the σ* orbital for this bond to lower energy. The appearance of a "new" peak at 285.5 eV upon surface reaction could then be the result of a shifting of an existing σ* resonance to a lower energy; this peak may well be hidden under the features assigned to the C–H transitions near 287.8 eV in the DMCd physisorbed spectra (Fig. 2a). This argument is supported by the increased peak width in the 287.8 eV feature in the physisorbed spectra when compared with the same feature in the chemisorbed spectrum.

In order to justify the above assignments we have compared spectral assignments in the literature where similar elements are involved in carbon bonds. For example, our 287.8 eV feature is at a very similar energy to a carbon K-shell transition assigned to a σ* S–C orbital in thiophene [28], raising the possibility that some methyl groups have become attached to sulfur. All of our previous mechanistic studies of this ALE process suggest that the direct bonding of methyl groups to the group VI component is unlikely and any possible surface termination involving this type of bond would violate the electron counting rules for stable surface reconstructions [29]. Unfortunately, in the absence of carbon K-edge spectra on suitable

model compounds and/or calculations of unoccupied orbital energies for the core-hole states, it is difficult to completely rule out alternative assignments.

Finally, returning to the NEXAFS data of multilayer DMCd, a weak shoulder-like feature at 285.5 eV is seen in the DMCd spectrum. An analysis of the edge jump heights shows that this feature is consistent with a chemisorbed layer of dissociated DMCd submerged under a physisorbed layer on the substrate at liquid N_2 temperature. The carbon K-edge jump in Fig. 2b is taken to represent 1 ML of methyl groups, as expected for room-temperature dosing of DMCd. By comparison, the edge jump for multilayer physisorption, Fig. 2a, is three times higher, indicating that about four times as much carbon is present. Our TPD studies show that partial reaction of DMCd occurs in the first monolayer, even at low temperature (see Fig. 4). The low intensity of the multilayer 285.5 eV peak would then be attributable to the screening of the chemisorbed resonance by approximately three overlayers of physisorbed DMCd and its location next to the tail of the more intense C–H peak at 287.8 eV. It would be desirable to repeat the physisorbed DMCd measurements using a much longer dosing time to insure that the feature at 285.5 eV will be completely suppressed.

In summary, the NEXAFS results from carbon K-edge features are consistent with a binary reaction sequence mechanism where reaction of DMCd with the bare surface or a succeeding group VI terminated surface ends with a methyl-terminated surface; subsequence dosing of this surface with H_2S desorbs the methyl groups probably in the form of CH_4.

3.2. Sulfur L-edge spectra from the adsorbed or grown surface layers

In a similar series of experiments, NEXAFS spectra were obtained at the sulfur L-edge in an attempt to prove the nature of the sulfur species present at various growth stages and to probe the composition of the thicker epitaxial CdS produced by this process. NEXAFS spectra were measured for physisorbed H_2S multilayers, chemisorbed H_2S-reacted surfaces, and annealed films containing an integral number of bilayers. These data are presented in Figs. 5 and 6.

3.2.1. Surface reaction studies

Curve (a) in Fig. 5 shows a spectrum measured after the surface has been covered with physisorbed multilayers of H_2S at liquid nitrogen temperature; again, as in the case for the DMCd experiments, the molecularly adsorbed nature of the film had been confirmed by TPD measurements. This spectrum shows two prominent near-edge peaks located at 165.2 and 166.4 eV, and a distinct shoulder at 164.4 eV. Similar features have been obtained from near-edge spectroscopy on gas-phase H_2S except that the isolated molecule has narrower linewidths than our condensed phase data [30]. In the gas-phase data, the three peaks were interpreted as arising from the overlapping

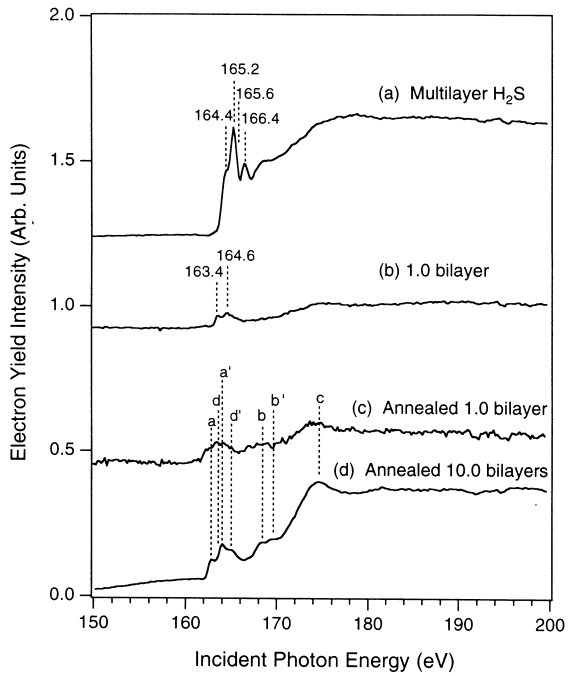

Fig. 5. Examples of sulfur L-edge NEXAFS spectra. Spectrum (a) is a reference spectrum of multilayer H_2S deposited on the substrate at low temperature. In (b), one full bilayer of CdS has been deposited by ALE. Changes occur in the spectra upon annealing to 275°C, as shown in (c). The features observed in (c) persist in (d), where growth has been extended to 10 bilayers, followed by 275°C annealing. Assignments are discussed in the text.

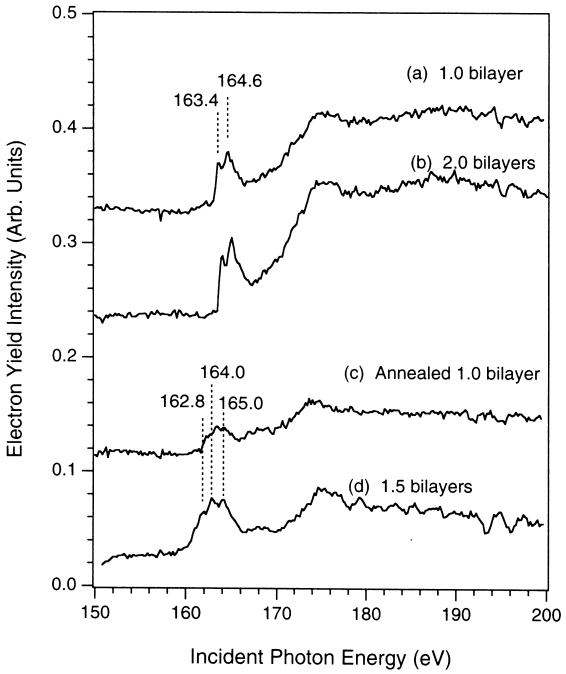

Fig. 6. Sulfur L-edge NEXAFS spectra for the first two bilayers of CdS growth. Spectra (a) and (b) are taken from 1.0 and 2.0 bilayer surfaces and have essentially the same features. The height of the step edge in (b) is about twice that in (a). When the 1.0 bilayer surface is annealed we obtained spectrum (c), which has similar features to the spectrum obtained following 1.5 bilayers of growth, (d).

of the four transitions from the sulfur spin–orbit-split $L_{II,III}$ levels, split by 1.2 eV [31], to the unoccupied $3b_2$ and $6a_1$ molecular orbitals, each transition with differing relative intensities. These transitions correspond to our features at (166.4 eV, 165.6 eV) and (165.2 eV, 166.4 eV), all of which lie below the sulfur $2p_{3/2}$ IP, which has been reported to be 170.2 eV [17]. In H_2S the lowest energy unoccupied orbitals are the $3b_2$ and $6a_1$ antibonding σ^* valence shell orbitals which lie below the Rydberg orbitals [32]. The ($3b_2$) orbital has sulfur (3p) and hydrogen (1s) character, the ($6a_1$) orbital has a stronger valence character involving the sulfur (3s, 3p, 3d) and H(1s) orbitals [33]. Two Rydberg series at the higher energy side of the spectrum, which are clearly seen in the gas-phase spectra [30], are not evident here. Again, this result is reasonable given that large, diffuse Rydberg orbitals tend to broaden into the band structure of a solid upon chemisorption or solidification, reducing their prominence when compared to the gas-phase spectra [34].

Dosing of a CH_3-terminated surface at room temperature resulted in a very different NEXAFS signature than that shown in Fig. 5a. First note that room-temperature exposure of a clean $c(2\times2)$ ZnSe surface with H_2S yields no sulfur L-edge spectral feature. However, if a surface consisting of metal–CH_3 termination was dosed with H_2S, new sulfur features were seen. Spectrum (b) in Fig. 5, taken from the surface after one complete dosing cycle, shows these features, i.e. two pre-edge peaks at 163.4 and 164.6 eV. The separation of these two peaks is 1.2 eV which is again consistent with the sulfur $L_{II,III}$ spin–orbit splitting reported for the isolated molecule. The features observed for the chemisorbed species are clearly different from those for the physisorbed multilayers of H_2S, indicating some change in the nature of the chemical bonding of sulfur.

Similar results were observed when H_2S is dosed onto still methyl-terminated but thicker epilayers. Fig. 6 shows the sulfur L-edge features at each reaction step for the first two bilayers of growth. The spectra taken from one bilayer and two bilayer CdS surfaces, Fig. 6a and 6b, are characterized by the same two peaks (16.3.4 eV, 164.6 eV). These results indicate that in each case identical reactions occur and that sulfur–hydride terminated surfaces are formed. Comparison of the step edge heights suggests that the surface concentration in Fig. 6b is around twice that in Fig. 6a, a result consistent with the layers each picking up an entire monolayer of sulfur from the dosing.

Separate TPD data (see Fig. 7), and the known reactivity of H_2S with DMCd, suggest that when a metal–methyl terminated surface is dosed with H_2S, a hydrogen-terminated sulfur monolayer is produced. However, since to our knowledge no NEXAFS spectra of M–SH species have been reported in the literature (though occupied bands have been derived for Mo–SH [35]), it is not possible to use NEXAFS to provide an unambiguous assignment of the surface terminating species. If an "as-grown" bilayer surface was terminated with sulfur hydride, the metal–SH bond is likely to result in an energy shift and a change in the

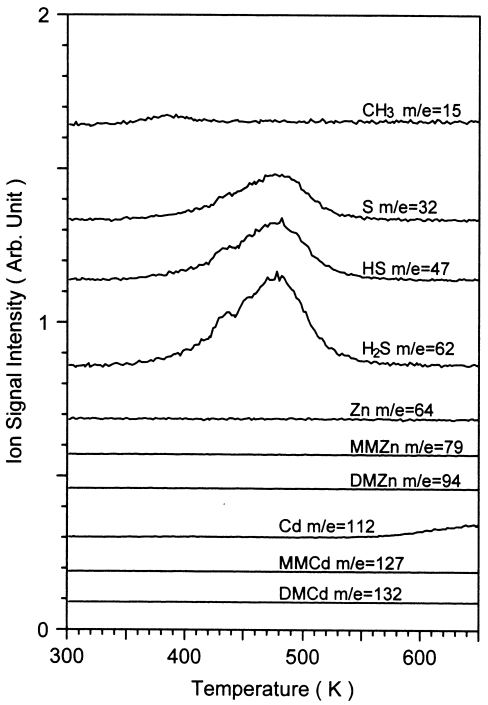

Fig. 7. TPD spectra taken following the dosing of a methyl-terminated surface with H_2S at room temperature. The reaction of H_2S with the surface appears to remove all of the methyl groups, with only sulfur-containing fragments desorbing near 480 K.

symmetry of molecular orbitals involved when compared to the equivalent orbitals in H_2S.

Annealing the presumably S–H terminated surface (Figs. 5c and 6c, denoted "1.0 bilayer") to a temperature of 275°C provides additional evidence for the existence of S–H termination. Heating to this temperature is known to be insufficient to desorb sulfur from bare CdS surfaces [14,15], but TPD measurements on an "as-grown" sample, shown in Fig. 7, indicate desorption of surface sulfur and hydrogen in the form of H_2S at a temperature less than 275°C. NEXAFS spectra of this surface, Figs. 5c and 6c, taken from heating to 275°C, result in replacement of the 163.4 and 164.6 eV features by a spectrum characteristic of bulk CdS (see below). It appears that a half monolayer of sulfur has desorbed in the form of H_2S, leaving behind a half monolayer of sulfur on the surface bound only to metal atoms.

3.2.2. NEXAFS spectra on the bulk film

Fig. 5d is a spectrum taken after the growth of a 10-bilayer CdS surface followed by annealing to 275°C to desorb the surface hydrogen. This spectrum has the identical features as the previously reported NEXAFS sulfur L-edge data for cubic CdS [11,12] thus suggesting the formation of bulk-like CdS. Assignment of the peaks near the sulfur $L_{II,III}$ absorption edge of cubic CdS are qualitatively interpreted based on the MO/energy band structure of bulk CdS. As suggested by our data and reported earlier for a crystalline bulk sample, the spectrum consists of several sharp peaks in the 162–170 eV region and a broad feature about 170 eV with a large absorption coefficient. This spectrum is believed to be a superposition of spectra due to the transitions from the L_{II} and L_{III} levels, which are separated by 1.2 eV, to s- or d-states in the conduction band. Referring to Fig. 8, these spectral peaks of the sulfur L-edge may be assigned as follows: peak a is assigned to transitions of S 2p electrons to S s-like (dominated by S 4s) states in the conduction band. Peak a is split into peaks a and a′, with a separation of about 1.2 eV, apparently due to the spin–orbit interaction of the S 2p electrons. Peaks b and c are at least partly attributable to transitions of S 2p electrons to empty S 3d bands in the CB. Since they have tetrahedral symmetry, the S 3d orbitals are split into e and t_2, and the e state is favored in energy over the t_2 state. Therefore, peak b is assigned to the transition of the S 2p electron to the e state, and peak c to the t_2 state (exhibiting shape resonances). Peak b is also split into b and b′ separated by about 1.2 eV. Peaks b and c are separated by about 6.0 eV which is in qualitative agreement with the crystal-field strength of cubic CdS [36].

Unlike transition metals, crystal-bonding interactions of Cd with sulfur are very weak since for Zn, Cd and Hg monosulfides, the Zn $3d^{10}$, Cd $4d^{10}$ and Hg $5d^{10}$ crystal-field bands lie below the metal–S bonding bands in the valence band rather than in the fundamental gap [37]. However, Cd 6s may interact with S 3s and S 3p orbitals as shown in Fig. 8 to form σ (bonding) and σ* (antibonding) orbitals. Peaks d and d′ may

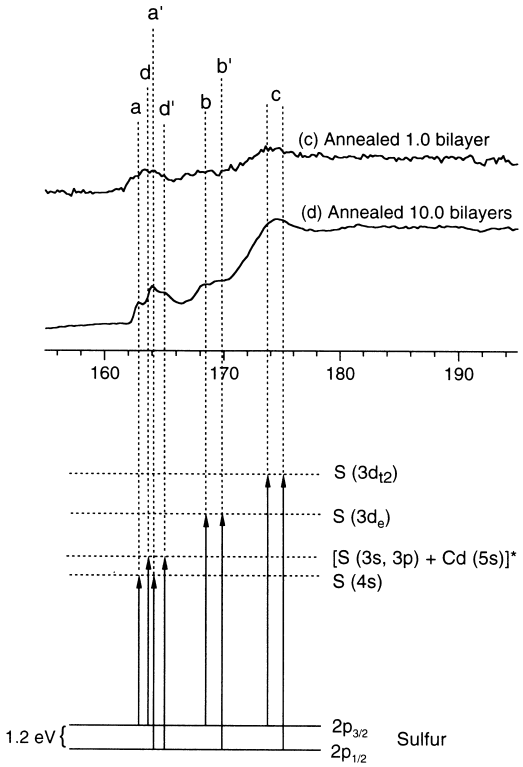

Fig. 8. Peak assignments of sulfur L-edge NEXAFS features for the grown CdS epilayers. These spectral features are similar to those reported in the literature for the cubic CdS [11,12].

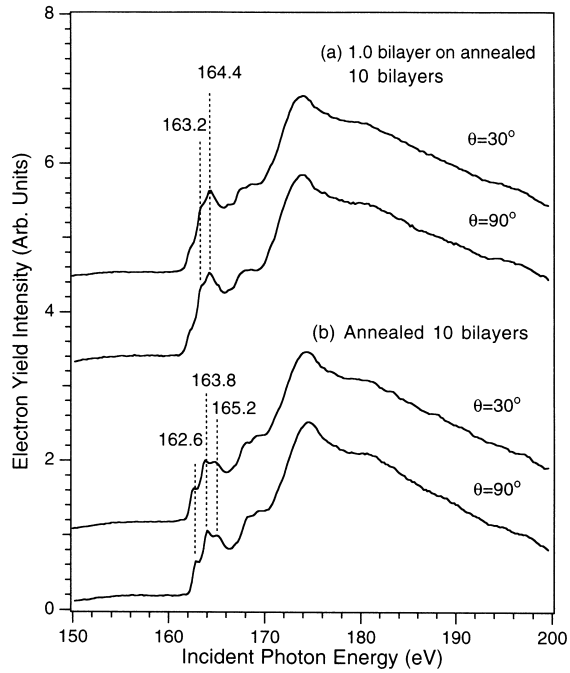

Fig. 9. The relative intensity of the observed sulfur L-edge spectral features appears to be insensitive to the incidence angle (and thus the polarization) of the synchrotron light. In the two top spectra, for incidence angles of 30° and 90°, the features associated with the S–H bonds at 164.4 and 163.2 eV have nearly identical heights when the step edge heights are made equal. The same is true for the annealed surfaces shown below, which correspond well with bulk CdS spectra.

originate from a transition from the sulfur L_{II}, L_{III} to this σ* antibonding orbital.

As shown in Fig. 6c and 6d, the spectra taken from the annealed 1.0 bilayer and as-grown 1.5 bilayer surfaces have the same features, with the features in the latter spectrum shifted to lower energies when compared to the 1.0 bilayer surface before annealing. The amount of sulfur detected for the annealed single bilayer is ~0.5 times that in the "as-grown" single bilayer. This result agrees with our TPD measurement (Fig. 7) which shows that hydrides desorb as H_2S leaving half of a monolayer of sulfur remaining on the surface. Finally, the amount of sulfur after 1.5 bilayers of growth is the same as that in the first bilayer, indicating that sulfur is not removed in the subsequent reaction with DMCd.

Fig. 7 also shows that no carbon-containing species are evolved when the "as-grown" presumably S–H terminated surfaces are heated. The detection of H_2S, HS and S near 470 K is attributed to desorption of H_2S, since the cracking patterning is the same as that measured for physisorbed H_2S in our system. H_2S is desorbed by the aforementioned restructuring to a half monolayer, S-terminated surface. Further TPD studies at various stages of the growth process are underway in our lab and will be reported in a further publication [18].

The top two traces in Fig. 9 show NEXAFS spectra at the S L-edge for a freshly grown (without annealing) bilayer deposited on an annealed 10-bilayer CdS surface. These spectra have been measured for two angles of the incoming radiation: $\theta = 30°$ (glancing) and $\theta = 90°$ (normal). Spectra at both angles show the re-appearance of features which have been attributed to the S–H σ* orbitals.

This indicates that the same reaction mechanism appears to operate even on an annealed thick CdS surface and a good quality CdS layer can be continuously grown with the binary reaction sequence.

In summary, the NEXAFS study of sulfur L-edge features also agrees with the "ideal" model of the surface reaction sequence (Fig. 1), in which H_2S reacts with the methyl-terminated surface, depositing a full layer of sulfur atoms, with each deposited atom passivated towards further reaction by hydrogen termination. The growth of the sulfur step edge with increasing epilayer thickness and the spectral signature of the grown layer are indicative of CdS growth.

3.3. Orientation of the adsorbed species

The polarized nature of synchrotron radiation can be used to determine surface molecular orientation because the intensity of a spectral feature is proportional to the square of the projection of the electric field vector ($\boldsymbol{E}$) of polarized light on the molecular transition dipole moment. For example, a methyl-terminated surface with carbon–surface bonds perpendicular to the surface should exhibit intensity changes in the C–Cd σ* features with a change in the incident angle of the radiation, e.g. the C–Cd σ* transition would be only observed at glancing incidence (where $\boldsymbol{E}$ has a large projection on the surface normal) and be absent at normal X-ray incidence ($\boldsymbol{E}$ vector parallel to the surface). A similar type of dependence would be expected for the transitions associated with S–H σ* orbitals on a sulfur–hydride terminated surface.

Several spectra for the carbon K-edge and sulfur L-edge were measured at both glancing 30° and normal 90° angles and then normalized to give the same step edge height. As shown in Fig. 10, no angular dependence in the carbon K-edge features was observed for DMCd dosed on a clean substrate (0.5 bilayer); the same invariance was also observed on 1.5 bilayers and 10.5 bilayers. Both the C–Cd σ* and C–H σ* intensities remained the same irrespective of the incidence angle. Similarly, no angular dependence of the S L-edge spectra was observed for spectra taken after the growth of 1.0 bilayers, 2.0 bilayers and 10.0 bilayers. Fig. 9 gives an example of the angular invariance observed in the sulfur spectra. This suggests two possibilities for the surface bond orientations, the first being that the bonds being probed are rather randomly oriented due to surface disorder. The other possibility is that the bonds associated with the σ* orbitals being probed are oriented near 54.7° with respect to the surface normal. A (100) truncation of the CdS (or ZnSe) crystal without reconstruction would have twofold rotational symmetry around the surface normal. Assuming that this is the structure of the surface that lies directly below the ligand-terminated surface, there are two equivalent possibilities for the azimuthal orientation of adsorbate domains. This places certain restrictions on the angular dependence of the intensities for σ-type resonance features resulting in relative intensities, I, that vary as [8,38]

$$I=\cos^2\theta\cos^2\alpha+\sin^2\theta\sin^2\alpha\cos^2\phi, \quad (1)$$

where θ is the polar angle of $\boldsymbol{E}$ with respect to the surface plane, α is the polar angle of the bond axis and ϕ is the azimuthal orientation of the bond axis relative to the incidence plane. Here we are

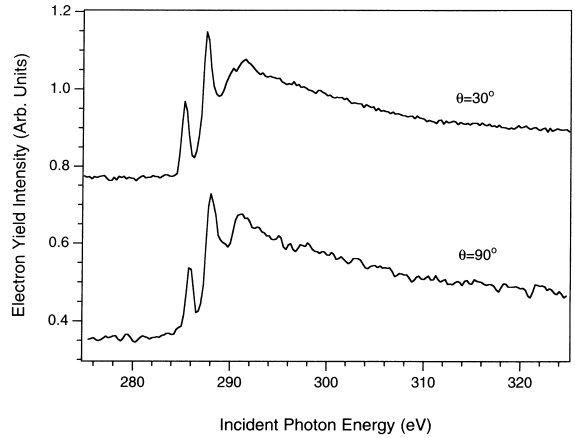

Fig. 10. Angular dependence of the carbon K-edge features for a methyl-terminated surface at the indicated incidence angles, shown here, as an example, spectra taken from 0.5 bilayers. Step edge heights have been normalized to be equal, as the absolute signal intensity varies with angle. As in the previous figure, the relative intensity of the spectral features is insensitive to the incidence angle.

assuming that $\boldsymbol{E}$ is highly polarized in the incidence plane.

While we could not make in situ LEED measurements at the synchrotron, subsequent measurements revealed that the substrate azimuthal orientations during the NEXAFS measurements were such that the rows of nearest neighbor atoms on the surface, which lie in the (011) and $(0\bar{1}1)$ directions, were at 45° to the incidence plane of the synchrotron radiation. Inspection of Eq. (1) reveals that the intensity will be independent of θ, the incidence angle, for $\alpha = 54.7°$, providing that the azimuthal orientation of the σ orbitals related to the transition are at $\phi = 45°$. Therefore, the observed angular invariance suggests that the bonds to capping ligands could lie in one of the planes defined by rows of nearest neighbor atoms and the substrate surface normal. With $\alpha = 54.7°$ this configuration is exactly what would be expected for the surface atoms to be tetrahedrally bound to the capping groups. Because we were unable to take further NEXAFS spectra at other azimuthal angles, a tetrahedral orientation for these bonds must be considered speculative; a new series of measurements at various azimuthal angles is planned for the near future. At this point the most likely explanation for the observed lack of angular dependence must be the absence of well-oriented bonds at the surface, possibly due to some level of surface roughness during growth, consistent with the step edge height and LEED measurements discussed above.

4. Summary

This paper describes the use of near-edge X-ray absorption spectroscopy and TPD studies to examine the surface chemistry in a layer-by-layer growth system. The results support a reaction sequence in which a single surface reaction both inserts an atomic constituent into a growing semiconductor crystalline layer and at the same time passivates the surface to further uptake of that constituent. Subsequent reaction with a precursor containing the other lattice constituent also removes the previous capping group, replacing it with another passivating layer. Self-limiting, layer-by-layer growth is achieved by cycling this process at room temperature. In this work we have successfully identified the nature of the passivating groups that are crucial to the operation of this scheme. Although some of our interpretations of the details of observations are tentative at present, e.g. the lack of a clear preferred orientation for the surface ligands, the measurements demonstrate clearly that NEXAFS can be used effectively for in situ measurement of the surface chemistry of growing films.

Acknowledgements

The author would like to thank the generous help of Brian DeVries and Andrew Mingino at the NSLS, and Andrew Teplyakov at New York University, with various aspects of the experimental work. Several discussions with Dr. Michael X. Yang were helpful in both the experimental and interpretive phases of this work. We acknowledge support by NSF contact #DMR-96-32456, with partial instrumentation support from DOE contact #FGO2-90ER14104.

References

[1] T. Suntola, M. Simpson, Atomic Layer Epitaxy, Chapman and Hall, New York, 1990.
[2] T. Suntola, J. Hyvarinen, Annu. Rev. Mater. Sci. 15 (1985) 117.
[3] C.H.L. Goodman, M.V.J. Pessa, Appl. Phys. 60 (1986) R65.
[4] S.M. George, O. Sneh, A.C. Dillon, M.L. Wise, A.W. Ott, L.A. Okada, J.D. Way, Appl. Surf. Sci. 82/83 (1994) 460–467.
[5] S.M. George, A.W. Ott, J.W. Klaus, J. Phys. Chem. 100 (31) (1996) 13121–13131.
[6] Y. Luo, D.A. Slater, M. Han, J.E. Moryl, R.M. Osgood Jr., Langmuir 14 (6) (1998) 1493–1499.
[7] Y. Luo, D.A. Slater, M. Han, J.E. Moryl, R.M. Osgood Jr., Appl. Phys. Lett. 71 (26) (1997) 3799–3801.
[8] J. Srohr, NEXAFS Spectroscopy, Springer-Verlag, Berlin, 1992.
[9] J.G. Chen, submitted to Surf. Sci. Rep.
[10] K.L. Brown, D.R. Evans, Inorg. Chem. 29 (1990) 2561.
[11] C. Sugiura, Y. Hayasi, H. Konuma, S.J. Klyono, Phys. Soc. Jpn. 31 (1971) 1748.
[12] D. Li, G.M. Bancroft, M.E. Fleet, X.H. Feng, K.H. Tan, B.X. Yang, J. Phys. Chem. Solids 55 (1994) 535.

[13] D.A. Fischer, J. Colbert, J.L. Gland, Rev. Sci. Instrum. 60 (1989) 1596.
[14] C.H. Park, D.J. Chadi, Phys. Rev. B 49 (1994) 16467–16473.
[15] L. Seehofer, G. Falkenberg, R.L. Johnson, V.H. Etgens, S. Tatarenko, D. Brun, B. Daudin, Appl. Phys. Lett. 67 (1995) 1680.
[16] D.A. Outka, J. Stohr, J. Chem. Phys. 86 (1988) 3539.
[17] W.L. Jolly, K.D. Bomben, C.J. Eyermann, At. Data and Nucl. Data Tables 31 (1984) 433.
[18] M. Han, Y. Luo, J.E. Moryl, R.M. Osgood, Jr., manuscript in preparation.
[19] Y. Luo, D.A. Slater, M. Han, J.E. Moryl, R.M. Osgood, Jr., manuscript in preparation.
[20] D.P. Woodruff, T.A. Delchar, Modern Techniques of Surface Science, Cambridge University Press, Cambridge, 1986.
[21] D. Briggs, M.P. Seah, Practical Surface Analysis, John Wiley and Sons Ltd., New York, 1983.
[22] P.J. Lasky, P.H. Lu, Y. Luo, D.A. Slater, R.M. Osgood, Jr., Surf. Sci. 364 (1996) 312–324.
[23] A.P. Hitchcock, S. Beaulieu, T. Steel, J. Stohr, F.J. Sette, Chem. Phys. 80 (1984) 3927.
[24] F. Sette, J. Stohr, A.P. Hitchcock, Chem. Phys. 81 (1984) 4906.
[25] M.N. Piancastelli, D.W. Lindle, T.A. Ferrett, D.A. Shirley, J. Chem. Phys. 86 (1987) 2765.
[26] P.J. Lasky, P.H. Lu, M.X. Lang, R.M. Osgood, Jr., B.E. Bent, P.A. Stevens, Surf. Sci. 336 (1995) 140–148.
[27] A.P. Hitchcock, Physica Scr. T31 (1990) 159.
[28] J. Stohr, J.L. Gland, E.B. Kollin, R.J. Koestner, A.L. Johnson, E.L. Muetterties, F. Sette, Phys. Rev. Lett. 53 (1984) 2161.
[29] W. Monch, Semiconductor Surfaces and Interfaces, Springer-Verlag, Berlin, 1995.
[30] W. Hayes, F.C. Brown, Phys. Rev. A 6 (1972) 21.
[31] W.H.F. Schwarz, Chem. Phys. 9 (1975) 157.
[32] W.H.F. Schwarz, Chem. Phys. 11 (1975) 217.
[33] S. Polezzo, M.P. Stabilini, M. Simonetta, Mol. Phys. 17 (1969) 609.
[34] A.P. Hitchcock, J.A. Horsley, J. Stohr, Chem. Phys. 85 (1986) 4835.
[35] J.A. Rodriguez, Surf. Sci. 278 (1992) 326.
[36] D.G. Sutherland, M. Kasrai, G.M. Bancroft, Z.F. Liu, K.H. Tan, Phys. Rev. B 48 (1993) 14989.
[37] J.A. Tossel, D.J. Vaughan, Inorg. Chem. 20 (1981) 3333.
[38] J. Stohr, D.A. Outka, Phys. Rev. B 36 (1987) 7891.